

# Gravitational wave background from Population III binary black holes consistent with cosmic reionization

Kohei Inayoshi<sup>1\*</sup>, Kazumi Kashiyama<sup>2</sup>, Eli Visbal<sup>1</sup>, Zoltán Haiman<sup>1</sup>

<sup>1</sup>*Department of Astronomy, Columbia University, 550 W. 120th Street, New York, NY 10027, USA*

<sup>2</sup>*Department of Astronomy; Theoretical Astrophysics Center; University of California, Berkeley, CA 94720, USA*

14 June 2016

## ABSTRACT

The recent discovery of the gravitational wave source GW150914 has revealed a coalescing binary black hole (BBH) with masses of  $\sim 30 M_{\odot}$ . Previous proposals for the origin of such a massive binary include Population III (PopIII) stars. PopIII stars are efficient producers of BBHs and of a gravitational wave background (GWB) in the 10–100 Hz band, and also of ionizing radiation in the early Universe. We quantify the relation between the amplitude of the GWB ( $\Omega_{\text{gw}}$ ) and the electron scattering optical depth ( $\tau_e$ ), produced by PopIII stars, assuming that  $f_{\text{esc}} \approx 10\%$  of their ionizing radiation escapes into the intergalactic medium. We find that PopIII stars would produce a GWB that is detectable by the future O5 LIGO/Virgo if  $\tau_e \gtrsim 0.07$ , consistent with the recent Planck measurement of  $\tau_e = 0.055 \pm 0.09$ . Moreover, the spectral index of the background from PopIII BBHs becomes as small as  $d \ln \Omega_{\text{gw}} / d \ln f \lesssim 0.3$  at  $f \gtrsim 30$  Hz, which is significantly flatter than the value  $\sim 2/3$  generically produced by lower-redshift and less-massive BBHs. A detection of the unique flattening at such low frequencies by the O5 LIGO/Virgo will indicate the existence of a high-chirp mass, high-redshift BBH population, which is consistent with the PopIII origin. A precise characterization of the spectral shape near 30–50 Hz by the Einstein Telescope could also constrain the PopIII initial mass function and star formation rate.

**Key words:** gravitational waves – black hole physics – stars: Population III

## 1 INTRODUCTION

Advanced LIGO (AdLIGO) announced the first direct detection of gravitational waves. The source, GW150914, is inferred to be a merging binary black hole (BBH) with masses of  $36_{-4}^{+5} M_{\odot}$  and  $29_{-4}^{+4} M_{\odot}$  at  $z = 0.09_{-0.03}^{+0.04}$  (Abbott et al. 2016c). The origin of such massive and compact BBHs are of astrophysical interest, and several pathways have been proposed for their formation. One channel is massive binary evolution in a metal-poor environment (Bond & Carr 1984; Belczynski, Bulik & Rudak 2004; Kulczycki et al. 2006; Dominik et al. 2012; Kinugawa et al. 2014, 2016, hereafter K14, K16; Belczynski et al. 2016), including rapid rotation and tides (Mandel & de Mink 2016), or assisted by accretion discs in active galactic nuclei (Bartos et al. 2016; Stone, Metzger & Haiman 2016). Alternative formation channels include stellar collisions in dense clusters (e.g. Portegies Zwart & McMillan 2000; O’Leary, Meiron & Kocsis 2016) or the collapse of rapidly-rotating massive stars (Loeb 2016). Given the estimated BBH merger rate of  $\sim 2 - 400 \text{ Gpc}^{-3} \text{ yr}^{-1}$  (Abbott et al.

2016d), these scenarios may be distinguished in the near future by their chirp mass distributions.

Another way to probe the star and BH formation history of the Universe by GWs is via the stochastic background (GWB) from numerous unresolved BBH mergers. Here we focus on one promising source, binary Population III (hereafter PopIII) stars formed in the early Universe at  $z \gtrsim 6$ . PopIII stars are thought to be massive (Bromm & Yoshida 2011, and references therein), and their binary fraction is expected to be at least as high as for present-day massive stars (e.g. Stacy & Bromm 2013). Thus PopIII stars may form massive BBHs effectively<sup>1</sup>. The vast majority of these BBHs merge at high redshifts and contribute to the GWB (Kowalska, Bulik & Belczynski 2012). A small minority merge after a delay comparable to the Hub-

<sup>1</sup> For the purposes of this paper, ‘PopIII’ refers to any stellar population with unusually high typical mass, forming predominantly at high redshift ( $z > 6$ ), and contributing to reionization at these redshifts. The IMF as a function of metallicity is poorly understood, and these properties may also be satisfied for an extreme ‘PopII’ stellar population, enriched to low, but non-zero metallicity (e.g.  $Z < 0.1 Z_{\odot}$ ; see Kowalska-Leszczynska et al. 2015; Belczynski et al. 2016).

\* E-mail: inayoshi@astro.columbia.edu

ble time, inside the detection horizon of AdLIGO. Recent PopIII binary population synthesis calculations predicted the event rate at  $z \simeq 0$  to be  $\sim 1 - 100 \text{ Gpc}^{-3} \text{ yr}^{-1}$ , and the chirp mass distribution to peak at  $\sim 30 M_{\odot}$  (K14; K16), in near-perfect agreement with GW150914.

PopIII stars are also efficient producers of ionizing radiation in the early Universe. Recently, the optical depth of the universe to electron scattering was inferred from the cosmic microwave background (CMB) anisotropies by the *Planck* satellite to be  $\tau_e = 0.066 \pm 0.016$  (Ade et al. 2015). This value is lower than previous estimates from *WMAP* (Komatsu et al. 2011), placing tight constraints on the formation history of PopIII stars (Visbal, Haiman & Bryan 2015, hereafter VHB15).

In this paper, we show that a PopIII BBH population that is consistent with the *Planck* optical depth measurement produces a GWB dominating over other BBH populations at 10 – 100 Hz. As a result, the stochastic GWB may be detectable sooner than previously expected. We also find that the spectral index of the GWB due to PopIII BBHs becomes significantly flatter at  $f \gtrsim 30 \text{ Hz}$  than the value  $d \ln \Omega_{\text{gw}} / d \ln f \approx 2/3$  generically produced by the circular, GW-driven inspiral of less massive and/or lower- $z$  BBHs (Phinney 2001). This flattening can not be mimicked by eccentric orbits or dissipative processes, and could be detected by the observing run O5 by AdLIGO/Virgo. Such a detection would provide robust evidence for a high-chirp-mass, high-redshift BBH population, and would yield information about the initial mass function (IMF) and star formation rate (SFR) of PopIII stars, and about cosmic reionization.<sup>2</sup>

## 2 MASSIVE BINARY FORMATION RATE AT HIGH-REDSHIFTS

### 2.1 PopIII stars ( $Z = 0$ )

PopIII stars are the first generation of stars in the Universe, beginning to form from pristine gas in mini-halos with masses of  $10^{5-7} M_{\odot}$  at redshifts  $z \sim 20 - 30$ . These stars are likely to be massive, because of inefficient cooling via molecular hydrogen ( $\text{H}_2$ ), resulting in a top-heavy IMF covering the mass range  $\sim 10 - 300 M_{\odot}$  (e.g. Hirano et al. 2014). Massive PopIII stars produce a strong Lyman-Werner (LW) radiation background, which dissociates  $\text{H}_2$  in mini-halos and suppresses subsequent star formation (e.g. Haiman, Rees & Loeb 1997). Including this self-regulation, the history of early star-formation has been investigated in semi-analytical studies (e.g. Haiman, Abel & Rees 2000; Sobacchi & Mesinger 2013) and in cosmological simulations (e.g. Ricotti, Gnedin & Shull 2002; Ahn et al. 2012).

The *Planck* measurement of the optical depth from the CMB ( $\tau_e = 0.066 \pm \Delta\tau_e$ , where  $\Delta\tau_e = 0.016$  is the  $1\sigma$  error; Ade et al. 2015) tightly constrains the PopIII star formation history. VHB15 estimated an upper limit on the total mass density of PopIII stars as  $\rho_{*III} \sim 10^5 M_{\odot} \text{ Mpc}^{-3}$ , consistent

<sup>2</sup> As this paper was being completed, we became aware of a recent preprint (Hartwig et al. 2016), which presents a more conservative estimate for the PopIII SFR and the corresponding GW emission. We here highlight the possibility of a higher PopIII SFR and GWB, which are still consistent with the *Planck* results.

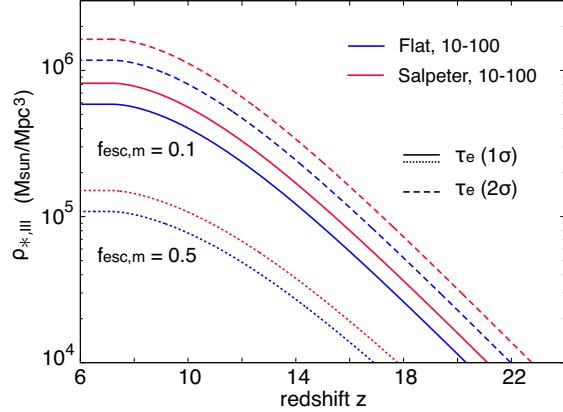


**Figure 1.** Cumulative (comoving) mass density of PopIII stars consistent with the *Planck* optical depth measurement from the CMB for two different IMFs: flat (blue) and Salpeter (red) with 10 – 100  $M_{\odot}$ . The optical depth is set to  $\tau_e = 0.066 + 0.016$  ( $1\sigma$ ; solid and dotted) and  $0.066 + 0.032$  ( $2\sigma$ ; dashed), respectively. Two cases with  $f_{\text{esc},m} = 0.1$  (solid and dashed) and 0.5 (dotted) are shown. At  $z \lesssim 8$ , PopIII star formation is shut down and the cumulative mass density saturates (see Eq. 1).

with the *Planck* result. They assumed a top-heavy IMF, with PopIII stars as massive as  $\sim 200 M_{\odot}$ , for which the number of H-ionizing and LW photons per stellar baryon are both  $\eta_{\text{ion}} \simeq \eta_{\text{LW}} \simeq 8 \times 10^4$ ; the escape fraction of ionizing photons from mini-halos was assumed to be  $f_{\text{esc},m} = 0.5$ .

We explore the dependence of  $\rho_{*III}$  on  $\eta_{\text{ion(LW)}}$ ,  $f_{\text{esc},m}$  and  $\tau_e$ . We consider two cases for a flat and a Salpeter IMF with 10 – 100  $M_{\odot}$ . The ionizing photon number per baryon is  $\eta_{\text{ion}} = 7.1 (5.1) \times 10^4$  for the flat (Salpeter) IMF (Schaerer 2002). Note that the value of  $\eta_{\text{ion}}$  is almost constant for a higher maximum mass of the IMF with  $M_{\text{max}} > 100 M_{\odot}$ . We assume  $\eta_{\text{ion}} = \eta_{\text{LW}}$ , which is a good approximation for these IMFs. We consider two values of the escape fraction,  $f_{\text{esc},m} = 0.1$  and 0.5. The higher value corresponds to mini-halos with  $10^{5-6} M_{\odot}$  (Kitayama et al. 2004), while the lower value corresponds to more massive halos with  $\gtrsim$  a few  $\times 10^7 M_{\odot}$  (Wise et al. 2014). In fact, the typical mass of halos forming PopIII stars is  $\simeq 10^{7-8} M_{\odot}$  at  $z \simeq 10$ , because once a LW background develops it disables  $\text{H}_2$  cooling in smaller halos. We thus adopt  $f_{\text{esc},m} = 0.1$  as our fiducial model.

Fig. 1 shows the cumulative (comoving) mass density of PopIII stars for different IMFs and escape fractions. All other model ingredients, apart from an overall normalization of the SFR, follow the fiducial model of VHB15. The normalization is chosen to produce an optical depth of  $\tau_e = 0.066 + \Delta\tau_e$  (solid and dotted curves) and  $0.066 + 2\Delta\tau_e$  (dashed curve). In all cases, the mass density of PopIII stars is saturated at  $z \lesssim 8$ , where PopIII star formation is shut down because of LW feedback, metal enrichment and reionization. The saturated value can be given approximately by

$$\rho_{*III} \simeq 8.2 \times 10^5 M_{\odot} \text{ Mpc}^{-3} \times \left( \frac{\eta_{\text{ion}}}{5 \times 10^4} \right)^{-1} \left( \frac{f_{\text{esc},m}}{0.1} \right)^{-1} \left( \frac{\tau_e - 0.066}{\Delta\tau_e} \right), \quad (1)$$

for the range we consider here. Note that K14 estimated the GW event rate from PopIII binaries adopt-

ing a higher comoving mass density of  $\rho_{*,\text{III}} \simeq 2 \times 10^6 M_\odot \text{Mpc}^{-3}$  (de Souza, Yoshida & Ioka 2011).

Next, we estimate the number density of massive PopIII binary stars which potentially evolve into PopIII BBHs. The distribution function of the mass ratio  $q \equiv M_2/M_1$  of binary stars is assumed to be  $\Phi(q) = \text{const}$ , where  $M_{1(2)}$  is the mass of the primary (secondary) star. This distribution is consistent with the slope  $d \ln \Phi / d \ln q = -0.1 \pm 0.6$ , observed for present-day massive binary stars (Sana et al. 2012). The mass ratio range for a fixed  $M_1$  is  $q_{\text{min}} (= M_{\text{min}}/M_1) \leq q \leq q_{\text{max}} (= M_{\text{max}}/M_1)$ . Thus, the number fraction of stars which form massive binaries with  $M_{1(2)} \geq M_{\text{crit}} = 25 M_\odot$ , above which a star is assumed to collapse into a BH (Heger & Woosley 2002), is estimated for a given IMF as

$$f_{\text{MB}} = \frac{\int_{M_{\text{crit}}}^{M_{\text{max}}} dM_1 \int_{q_{\text{crit}}}^{q_{\text{max}}} dq \Phi(q) \frac{dN}{dM_1}}{\int_{M_{\text{min}}}^{M_{\text{max}}} dM_1 \int_{q_{\text{min}}}^{q_{\text{max}}} dq \Phi(q) \frac{dN}{dM_1}},$$

$$= \frac{M_{\text{max}} - M_{\text{crit}}}{M_{\text{max}} - M_{\text{min}}} \begin{cases} \frac{\ln(M_{\text{max}}/M_{\text{crit}})}{\ln(M_{\text{max}}/M_{\text{min}})} & \text{for } \alpha = 0, \\ \frac{M_{\text{crit}}^{-\alpha} - M_{\text{max}}^{-\alpha}}{M_{\text{min}}^{-\alpha} - M_{\text{max}}^{-\alpha}} & \text{for } \alpha \neq 0, \end{cases} \quad (2)$$

where  $q_{\text{crit}} = M_{\text{crit}}/M_1$ . For the flat ( $\alpha = 0$ ) and Salpeter ( $\alpha = 2.35$ ) IMF with  $10 - 100 M_\odot$ , we estimate  $f_{\text{MB}} \simeq 9.3 \times 10^{-2}$  and  $0.5$ , respectively. From Eqs. (1) and (2), the number density of the massive binaries is estimated as

$$N_{\text{MB,III}} = \frac{\rho_{*,\text{III}}}{\langle M_* \rangle} \frac{f_{\text{bin}}}{1 + f_{\text{bin}}} f_{\text{MB}}$$

$$= 1.6 \times 10^3 \text{Mpc}^{-3} \left( \frac{\eta_{\text{ion}}}{50000} \right)^{-1} \left( \frac{f_{\text{esc,m}}}{0.1} \right)^{-1}$$

$$\times \left( \frac{\langle M_* \rangle}{20 M_\odot} \right)^{-1} \left( \frac{f_{\text{bin}}/0.7}{1 + f_{\text{bin}}/0.7} \right) \left( \frac{f_{\text{MB}}}{0.1} \right), \quad (3)$$

where  $\langle M_* \rangle$  is the average mass of single stars,  $f_{\text{bin}} \equiv N_{\text{binary}}/N_{\text{single}}$  is the binary fraction, and the fiducial  $f_{\text{bin}} = 0.7$  is based on the binary fraction  $0.69 \pm 0.09$  measured for present-day massive stars (Sana et al. 2012). Thus, the number density of PopIII BBHs is estimated as  $N_{\text{MB,III}} \simeq 2.7 (1.4) \times 10^3 \text{Mpc}^{-3}$  for the flat (Salpeter) IMF.

Fig. 2 shows the number of massive binaries per ionizing photon, a quantity directly connecting the GWB to reionization, from PopIII stars for the flat (blue) and Salpeter (red) IMF with  $5 M_\odot \leq M_{\text{min}} \leq 25 M_\odot$ . Note that stars with  $M > 25 M_\odot$  contribute both BBHs and ionizing photons, while stars in the range  $5 - 25 M_\odot$  add significant ionizing photons without any additional BBHs. As long as PopIII stars are massive, with  $M_{\text{min}} \gtrsim 10 M_\odot$ , our results are relatively insensitive to the slope of the IMF (less than a factor of two). However, if  $M_{\text{min}} \lesssim 10 M_\odot$ , normalizing the ionizing emissivity to match the *Planck* optical depth implies fewer massive binaries, and the precise value also depends more strongly on the IMF slope.

## 2.2 PopII stars ( $Z \sim 0.1 Z_\odot$ )

Population II (PopII) stars are formed in metal-enriched gas clouds once supernovae of massive PopIII stars have produced heavy elements. Because metal/dust cooling is more efficient than  $\text{H}_2$  cooling, the IMF of PopII stars is expected

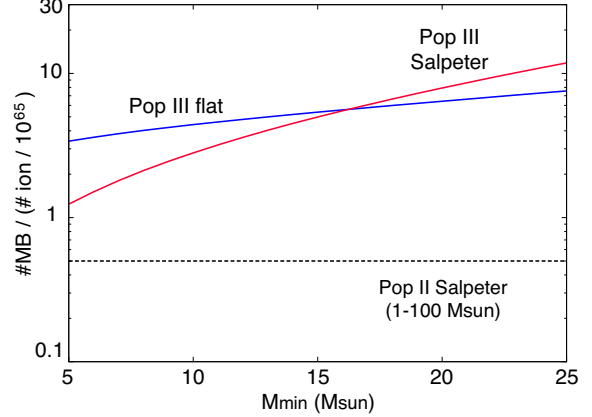


**Figure 2.** The ratio of the number of massive BH binaries to the number of ionizing photons for a flat (blue) and Salpeter (red) PopIII IMF with  $5 M_\odot \leq M_{\text{min}} \leq 25 M_\odot$  and  $M_{\text{max}} = 100 M_\odot$ . For reference, the ratio for a Salpeter IMF of PopII stars with  $1 M_\odot \leq M \leq 100 M_\odot$  is shown (black dashed). All curves assume a stellar binary fraction of  $f_{\text{bin}} = 0.7$ . PopIII stars with  $M_{\text{min}} \gtrsim 10 M_\odot$  produce an  $\sim$  order of magnitude more BH binaries.

to be less top-heavy (e.g. Omukai et al. 2005). We assume that once metal enrichment has occurred, PopII stars form with  $\simeq 0.1 Z_\odot$ , although the precise value of this metallicity does not significantly affect our results.

Observations of high-redshift galaxies provide estimates of the stellar mass density (e.g. Pérez-González et al. 2008), which are consistent with cosmological simulations (e.g. Vogelsberger et al. 2013). At  $z \sim 3$ , the (comoving) stellar mass density is  $\rho_* \simeq 3 \times 10^7 M_\odot \text{Mpc}^{-3}$ . Assuming a Salpeter IMF with  $1 - 100 M_\odot$  and the mass-ratio distribution  $\Phi(q) = \text{const}$ , the number fraction of massive binaries with  $M_{1(2)} \geq M_{\text{crit}} = 25 M_\odot$  is  $f_{\text{MB}} = 3.8 \times 10^{-4}$ , and the number density of PopII BBHs is  $N_{\text{MB,II}} \simeq 1.5 \times 10^3 \text{Mpc}^{-3}$  (for  $f_{\text{bin}} = 0.7$ ). The number density of PopII and PopIII binaries is almost identical, even though the total stellar mass in PopII stars is much higher than in PopIII stars. For comparison, in Fig. 2 we also show the ratio of the number of massive binaries to ionizing photons for a PopII Salpeter IMF with  $1 - 100 M_\odot$  (dashed), where  $\eta_{\text{ion}} = 8710$  is assumed (Samui, Srianand & Subramanian 2007). This shows that PopII stars produce fewer BBHs per ionizing photon. Nevertheless, with the normalization above, we find that PopII stars produce an ionizing background of  $J_{\nu,\text{bg}} \simeq 5 \times 10^{-22} \text{erg s}^{-1} \text{cm}^{-2} \text{Hz}^{-1} \text{sr}^{-1}$  (in physical units), consistent with  $\approx 50\%$  of the background measured at  $z \sim 3$  (e.g. Steidel, Pettini & Adelberger 2001). We note that 90% of present-day stars form between  $0 < z < 3$ ; however, the more recent, more metal-rich generations at  $z < 3$  are not expected to dominate the GWB, assuming a merger rate of BBHs by e.g., Dominik et al. (2013).

## 3 GRAVITATIONAL WAVES FROM POPIII BINARY BLACK HOLE MERGERS

We next consider the evolution of massive binaries to estimate the merger rate of PopIII BBHs. As discussed by K14 in the context of their population synthesis model, most

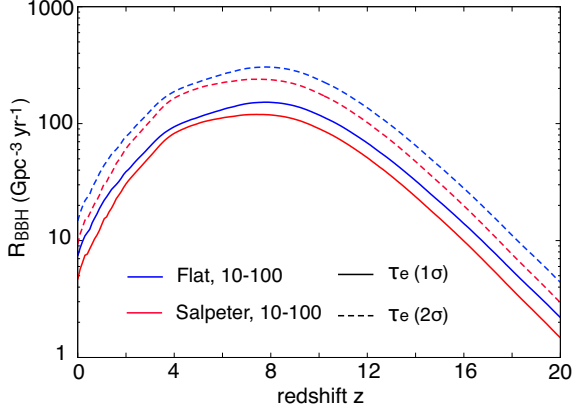


**Figure 3.** Merger rate of PopIII BBHs for different assumed IMFs, as in Fig. 2. The data is taken from K14, but renormalized to be consistent with the electrons scattering optical depth  $\tau_e$  measured by *Planck* within the  $1\sigma$  (solid) and  $2\sigma$  (dashed) error (Eq. 1 with  $f_{\text{esc,m}} = 0.1$  and  $\eta_{\text{ion}} = 5 \times 10^4$ ).

massive PopIII binaries can evolve into BBHs because in the absence of metals (1) mass loss from the metal-free surface is suppressed, and (2) stars are compact, which suppresses the deleterious effects of stellar binary interactions and mergers. Furthermore, PopIII stars with  $\sim 30 M_\odot$  are unlikely to evolve into red giants (Marigo et al. 2001), and as a result, the typical chirp mass of PopIII BBHs is  $\langle M_{\text{chirp}} \rangle \simeq 30 M_\odot$  for both a flat and a Salpeter IMF with  $10 - 100 M_\odot$  (K14).

By comparison, when massive PopII stars experience strong mass loss, they go through a red giant phase. These effects would reduce the average PopII BBH chirp mass to  $\sim 10 M_\odot$  (Kowalska-Leszczynska et al. 2015), and suppress the formation of BBHs somewhat (Belczynski et al. 2010). Furthermore, the average separation of PopII BBHs which escape mergers during the red giant phases would be larger, and their GW inspiral time is longer, so that only a few percent merges within a Hubble time (K14).

Fig. 3 shows the evolution of the PopIII BBH merger rate  $R_{\text{BBH}}$  for the flat (blue) and Salpeter (red) IMF with  $10 - 100 M_\odot$ . The distribution of the initial binary separation  $a$  is assumed to be  $\propto a^{-1}$  (Abt 1983). The rates are normalized using the cumulative mass density of PopIII stars consistent with the *Planck*  $\tau_e$  within the  $1\sigma$  (solid) and  $2\sigma$  (dashed) error (Eq. 1 for  $f_{\text{esc,m}} = 0.1$  and  $\eta_{\text{ion}} = 5 \times 10^4$ ), with the redshift-dependence of the SFR following de Souza, Yoshida & Ioka (2011). The rates peak between  $z \approx 4 - 10$  at  $\gtrsim 100 \text{ Gpc}^{-3} \text{ yr}^{-1}$ , with most merging PopIII BBHs unresolved by AdLIGO/Virgo, and with  $\gtrsim 10^{10}$  PopIII BBHs contributing to a strongly redshifted GWB over five years. The merger rates decrease toward low redshift once PopIII star formation is quenched. However, the rate remains as high as  $R_{\text{BBH}} \simeq 10 \text{ Gpc}^{-3} \text{ yr}^{-1}$  even at  $z \simeq 0$ , because BBHs with suitable initial separations take a Hubble time to merge. For a massive  $30 + 30 M_\odot$  circular BBH with an initial separation of  $\sim 0.2 \text{ AU}$ , the GW inspiral time is 10 Gyr (Peters & Mathews 1963). Note that the merging rate is consistent with  $\sim 2 - 400 \text{ Gpc}^{-3} \text{ yr}^{-1}$  inferred from GW150914 (Abbott et al. 2016d).

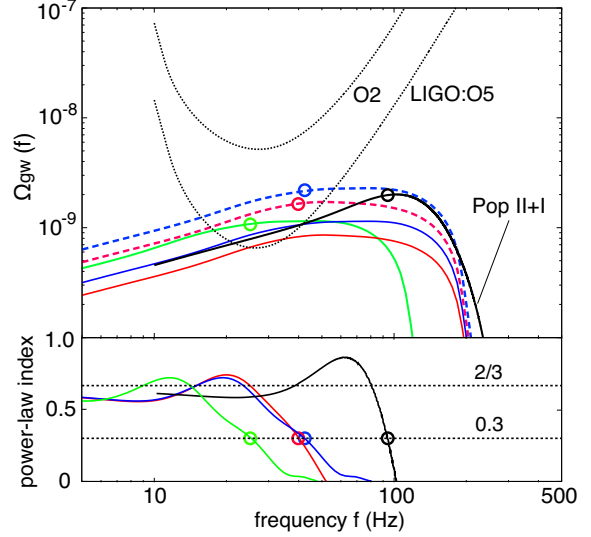


**Figure 4.** *Top:* spectra of GWB produced by PopIII BBHs for the same IMFs,  $f_{\text{esc,m}}$  and  $\tau_e$  as in Fig. 3 (blue and red curves). We assume binaries with the average chirp mass of  $\langle M_{\text{chirp}} \rangle = 30 M_\odot$  on circular orbits. The background expected from all unresolved PopII+PopI BBHs is shown for reference (solid black curve, Abbott et al. 2016b, their fiducial model). Black dotted curves show the expected sensitivity of AdLIGO/Virgo in the observing runs O2 and O5. The green solid curve is the same as the blue solid curve, but with a higher chirp mass of  $\langle M_{\text{chirp}} \rangle = 50 M_\odot$  and with a lower merging rate by a factor of  $3/5$ . *Bottom:* the spectral index; open circles mark the frequencies above which  $\alpha < 0.3$ .

We estimate the spectrum of the PopIII GWB as

$$\rho_c c^2 \Omega_{\text{gw}}(f) = \int_{z_{\text{min}}}^{\infty} \frac{R_{\text{BBH}} dt}{1+z} \left( f_r \frac{dE_{\text{gw}}}{df_r} \right) \Big|_{f_r=f(1+z)} dz \quad (4)$$

(Phinney 2001), where  $f$  and  $f_r$  are the GW frequencies observed at  $z = 0$  and in the source's rest frame, respectively, and  $\rho_c$  is the critical density of the Universe. We set the minimum redshift to  $z_{\text{min}} = 0.28$ , the detection horizon of AdLIGO/Virgo. The GW spectrum from a coalescing BBH is given by

$$\frac{dE_{\text{gw}}}{df_r} = \frac{(\pi G)^{2/3} M_{\text{chirp}}^{5/3}}{3} \begin{cases} f_r^{-1/3} \mathcal{F}_{\text{PN}} & f_r < f_1, \\ \omega_m f_r^{2/3} \mathcal{G}_{\text{PN}} & f_1 \leq f_r < f_2, \\ \frac{\omega_r \sigma^4 f_r^2}{[\sigma^2 + 4(f_r - f_2)^2]} & f_2 \leq f_r < f_3, \end{cases} \quad (5)$$

where  $E_{\text{gw}}$  is the energy emitted in GWs,  $M_{\text{chirp}} \equiv (M_1 M_2)^{3/5} / (M_1 + M_2)^{1/5}$  is the chirp mass, and  $f_i$  ( $i = 1, 2, 3$ ) and  $\sigma$  are frequencies that characterize the inspiral-merger-ringdown waveforms,  $\omega_{m(r)}$  are normalization constants chosen so as to make the waveform continuous, and the Post-Newtonian correction factors of  $\mathcal{F}(\mathcal{G})_{\text{PN}}$  (Ajith et al. 2011). We assume that the BBHs have circular orbits because the PopIII BBHs should circularize by the time they move into the LIGO band (see Fig.3 in Abbott et al. 2016a). Note that the background spectrum in the inspiral phase scales with frequency as  $\Omega_{\text{gw}}(f) \propto f^{2/3}$ .

Fig. 4 shows spectra of the GWB produced by PopIII BBHs for the same IMFs,  $f_{\text{esc,m}}$  and  $\tau_e$  as in Fig. 3 (blue and red curves). For the two IMFs with  $10 - 100 M_\odot$  and a

flat mass ratio distribution, the typical merger is an equal-mass binary with a chirp mass of  $\langle M_{\text{chirp}} \rangle \simeq 30 M_{\odot}$  (K14; K16). For comparison, we show the background produced by all PopII/I BBHs (black solid curve), which typically merge at  $z \lesssim 2 - 4$  (Dominik et al. 2013; Abbott et al. 2016b). For all cases shown, the GWB from PopIII BBHs is higher than the expected sensitivity of the AdLIGO/Virgo detectors in the observing run O5 (black dotted curves). The typical chirp mass and redshift of PopIII BBHs are both higher than for PopII/I BBHs ( $\sim 30 M_{\odot}$  vs  $\sim 10 M_{\odot}$  and  $z \sim 8$  vs.  $z \sim 3$ ), causing the GW frequency to be redshifted. As a result, the spectrum in the AdLIGO/Virgo band becomes flatter than the canonical  $\Omega_{\text{gw}}(f) \propto f^{2/3}$  expected from lower-redshift and lower-mass PopII/I sources. Kowalska, Bulik & Belczynski (2012) also have noted the spectral flattening by assuming a different chirp mass distribution and a high PopIII SFR which is inconsistent with the Planck result and does not include important physics (e.g. LW feedback, metal enrichment and reionization). In the bottom panel, the open circles mark the frequencies above which the spectral index falls below 0.3; this critical frequency is  $\sim 40$  Hz, well inside the AdLIGO/Virgo band. The deviation could be detectable with  $S/N \sim 3$  in the O5 run (Abbott et al. 2016b). Note that PopII/I BBHs can produce such a significant flattening of the GWB spectrum at  $\sim 100$  Hz (black curve; see also Kowalska-Leszczynska et al. 2015 that show a similar flattening at  $\gtrsim 70 - 100$  Hz, depending on their models.) Although a sub-dominant population of massive PopII BBHs with  $\gtrsim 30 M_{\odot}$  would form, depending on a model of cosmic metal enrichment (Belczynski et al. 2016), the severe flattening requires the majority of such massive stars, as expected only in the PopIII model (although of course this remains uncertain). Finally, we increase the chirp mass to  $50 M_{\odot}$  to see its impact (green solid curve). In this case, the critical frequency shifts to  $\sim 25$  Hz, allowing the deviation of the spectral index to be measured more easily. The spectral shape near  $30 - 50$  Hz would be precisely observed by the Einstein Telescope (ET)<sup>3</sup> with the expected sensitivity of  $\Omega_{\text{gw}} \approx 10^{-10} - 10^{-11}$  at  $f \sim 30$  Hz.

#### 4 SUMMARY AND DISCUSSION

In this paper, we show that GW background produced by PopIII binary BHs can dominate other populations at  $10 - 100$  Hz, even considering tight constraints on PopIII star formation by the recent *Planck* optical depth measurement from the CMB. We also find that the spectral index of the background from PopIII BHs becomes significantly flatter at  $\gtrsim 30$  Hz than the canonical value of  $\approx 2/3$  expected from lower- $z$  and less-massive circular binaries.

As discussed in §2, massive PopIII stars are also sources of ionizing photons in the early Universe. Thus, future observations of reionization and high-redshift galaxies could yield constraints on the PopIII BBH scenario. Fig. 5 shows the amplitude of the PopIII GWB at  $f = 30$  Hz for different values of the CMB optical depth (red solid), assuming  $f_{\text{esc,m}} = 0.1$ , a flat IMF with  $10 - 100 M_{\odot}$  and  $\langle M_{\text{chirp}} \rangle = 30 M_{\odot}$ . For our fiducial case, the PopIII GWB

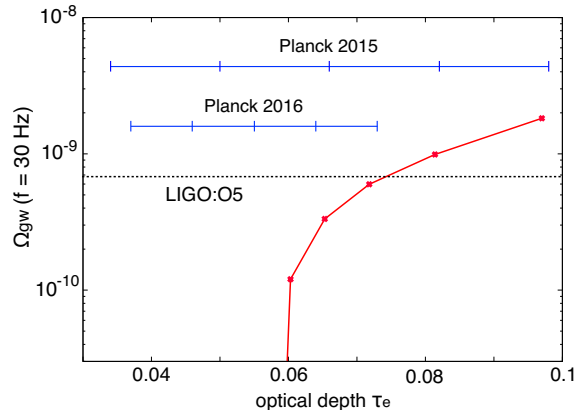


**Figure 5.** The PopIII GWB at  $f = 30$  Hz as a function of the CMB optical depth (red solid), for  $f_{\text{esc,m}} = 0.1$ , a flat IMF with  $10 - 100 M_{\odot}$  and  $\langle M_{\text{chirp}} \rangle = 30 M_{\odot}$ . For  $\tau_e \gtrsim 0.07$ , the PopIII GWB can be above the expected sensitivity of the future O5 AdLIGO/Virgo (dotted). The results of the *Planck* optical depth measurement with  $1\sigma$  and  $2\sigma$  errors are shown (Ade et al. 2015; Adam et al. 2016).

would be above the expected sensitivity of AdLIGO/Virgo in the observing run O5 (dotted) as long as  $\tau_e \gtrsim 0.07$ . However, for a small value of  $\tau_e \lesssim 0.06^4$ , ionizing photons from PopIII stars would contribute negligibly to reionization (e.g. Mitra, Choudhury & Ferrara 2015; VHB15)<sup>5</sup>. A detection of the PopIII GWB by the future observations (O5 AdLIGO/Virgo, KAGRA<sup>6</sup> and ET), if any, implies that the IMF of PopIII stars would be more top-heavy, where PopIII stars form more BBHs but produce less ionizing photons (see Fig. 2). The GWB (even an upper limit) would provide a useful constraint on the PopIII BBH scenario, combining with theoretical studies of high- $z$  star formation.

The origin of massive BBHs such as GW150914 is still uncertain. Future detections of multiple GW events with a BBH coalescence rate of  $R_{\text{BBH}} \sim 10 \text{ Gpc}^{-3} \text{ yr}^{-1}$  and a typical chirp mass of  $\sim 30 M_{\odot}$  would suggest a PopIII BBH scenario. In this case, the GWB could also be detectable, along with a significant flattening of the spectral index. There are three other effects which can cause a deviation of the spectral slope from the canonical value for circular, GW-driven, non-spinning inspirals: (i) environmental effects (interaction of the BHs with nearby gas and/or stars), (ii) high orbital eccentricities and (iii) high BH spins. The first two of these effects would generically steepen the spectral slope because environmental effects remove energy preferentially at large separations, and eccentricities move power from low to high frequencies. In principle, strong BH spins anti-aligned with the orbital angular momentum can flatten the spectrum significantly, but only at high frequencies near the merger (e.g.

<sup>4</sup> Recently, new values of  $\tau_e$  by *Planck* have been proposed as  $0.055 \pm 0.009$  and  $0.058 \pm 0.012$  ( $1\sigma$ ), respectively (Adam et al. 2016; Aghanim et al. 2016).

<sup>5</sup> A lower escape fraction of ionizing photons from PopII galaxies ( $f_{\text{esc,II}} < 0.1$ ) would allow a higher PopIII star (BBH) formation rate, however reducing this escape fraction prevents the completion of reionization by  $z = 6$ .

<sup>6</sup> <http://gwcenter.icrr.u-tokyo.ac.jp/en/>

<sup>3</sup> <http://www.et-gw.eu/etdsdocument>

Zhu et al. 2011). Therefore, the detection of a flattening of the spectral index of GWB at frequencies as low as 30 Hz would be a unique smoking gun of a high-chirp mass, high-redshift BBH population, as expected from PopIII stars.

## ACKNOWLEDGEMENTS

We thank Imre Bartos, Bence Kocsis, Tomoya Kinugawa, Tania Regimbau, David Schiminovich and Alberto Sesana for useful discussions. This work is partially supported by the Simons Foundation through the Simons Society of Fellows (KI), by NASA through an Einstein Postdoctoral Fellowship (KK), by the Columbia Prize Postdoctoral Fellowship in the Natural Sciences (EV) and by NASA grants NNX11AE05G and NNX15AB19G (ZH).

## REFERENCES

- Abbott B. P. et al., 2016a, *ApJL*, 818, L22  
 Abbott B. P. et al., 2016b, arXiv:1602.03847  
 Abbott B. P. et al., 2016c, *Physical Review Letters*, 116, 061102  
 Abbott B. P. et al., 2016d, arXiv:1602.03842  
 Abt H. A., 1983, *ARA&A*, 21, 343  
 Adam R. et al., 2016, arXiv:1605.03507  
 Ade P. A. R. et al., 2015, arXiv:1502.01589  
 Aghanim N. et al., 2016, arXiv:1605.02985  
 Ahn K., Iliev I. T., Shapiro P. R., Mellema G., Koda J., Mao Y., 2012, *ApJL*, 756, L16  
 Ajith P. et al., 2011, *Physical Review Letters*, 106, 241101  
 Bartos I., Kocsis B., Haiman Z., Márka S., 2016, arXiv:1602.03831  
 Belczynski K., Bulik T., Rudak B., 2004, *ApJL*, 608, L45  
 Belczynski K., Dominik M., Bulik T., O’Shaughnessy R., Fryer C., Holz D. E., 2010, *ApJL*, 715, L138  
 Belczynski K., Holz D. E., Bulik T., O’Shaughnessy R., 2016, arXiv:1602.04531  
 Bond J. R., Carr B. J., 1984, *MNRAS*, 207, 585  
 Bromm V., Yoshida N., 2011, *ARA&A*, 49, 373  
 de Souza R. S., Yoshida N., Ioka K., 2011, *A&A*, 533, A32  
 Dominik M., Belczynski K., Fryer C., Holz D. E., Berti E., Bulik T., Mandel I., O’Shaughnessy R., 2012, *ApJ*, 759, 52  
 Dominik M., Belczynski K., Fryer C., Holz D. E., Berti E., Bulik T., Mandel I., O’Shaughnessy R., 2013, *ApJ*, 779, 72  
 Haiman Z., Abel T., Rees M. J., 2000, *ApJ*, 534, 11  
 Haiman Z., Rees M. J., Loeb A., 1997, *ApJ*, 476, 458  
 Hartwig T., Volonteri M., Bromm V., Klessen R. S., Barausse E., Magg M., Stacy A., 2016, arXiv:1603.05655  
 Heger A., Woosley S. E., 2002, *ApJ*, 567, 532  
 Hirano S., Hosokawa T., Yoshida N., Umeda H., Omukai K., Chiaki G., Yorke H. W., 2014, *ApJ*, 781, 60  
 Kinugawa T., Inayoshi K., Hotokezaka K., Nakauchi D., Nakamura T., 2014, *MNRAS*, 442, 2963  
 Kinugawa T., Miyamoto A., Kanda N., Nakamura T., 2016, *MNRAS*, 456, 1093  
 Kitayama T., Yoshida N., Susa H., Umemura M., 2004, *ApJ*, 613, 631  
 Komatsu E. et al., 2011, *ApJS*, 192, 18  
 Kowalska I., Bulik T., Belczynski K., 2012, *A&A*, 541, A120  
 Kowalska-Leszczynska I., Regimbau T., Bulik T., Dominik M., Belczynski K., 2015, *A&A*, 574, A58  
 Kulczycki K., Bulik T., Belczyński K., Rudak B., 2006, *A&A*, 459, 1001  
 Loeb A., 2016, *ApJL*, 819, L21  
 Mandel I., de Mink S. E., 2016, *MNRAS*  
 Marigo P., Girardi L., Chiosi C., Wood P. R., 2001, *A&A*, 371, 152  
 Mitra S., Choudhury T. R., Ferrara A., 2015, *MNRAS*, 454, L76  
 O’Leary R. M., Meiron Y., Kocsis B., 2016, arXiv:1602.02809  
 Omukai K., Tsuribe T., Schneider R., Ferrara A., 2005, *ApJ*, 626, 627  
 Pérez-González P. G. et al., 2008, *ApJ*, 675, 234  
 Peters P. C., Mathews J., 1963, *Physical Review*, 131, 435  
 Phinney E. S., 2001, arXiv:0108028  
 Portegies Zwart S. F., McMillan S. L. W., 2000, *ApJL*, 528, L17  
 Ricotti M., Gnedin N. Y., Shull J. M., 2002, *ApJ*, 575, 49  
 Samui S., Srianand R., Subramanian K., 2007, *MNRAS*, 377, 285  
 Sana H. et al., 2012, *Science*, 337, 444  
 Schaerer D., 2002, *A&A*, 382, 28  
 Sobacchi E., Mesinger A., 2013, *MNRAS*, 432, 3340  
 Stacy A., Bromm V., 2013, *MNRAS*, 433, 1094  
 Steidel C. C., Pettini M., Adelberger K. L., 2001, *ApJ*, 546, 665  
 Stone N. C., Metzger B. D., Haiman Z., 2016, arXiv:1602.04226  
 Visbal E., Haiman Z., Bryan G. L., 2015, *MNRAS*, 453, 4456  
 Vogelsberger M., Genel S., Sijacki D., Torrey P., Springel V., Hernquist L., 2013, *MNRAS*, 436, 3031  
 Wise J. H., Demchenko V. G., Halicek M. T., Norman M. L., Turk M. J., Abel T., Smith B. D., 2014, *MNRAS*, 442, 2560  
 Zhu X.-J., Howell E., Regimbau T., Blair D., Zhu Z.-H., 2011, *ApJ*, 739, 86